# Independent Confirmation of the Pioneer 10 Anomalous Acceleration

Craig B. Markwardt,[*]

*Laboratory for High Energy Astrophysics,*

*NASA Goddard Space Flight Center,*

*Code 662, Greenbelt, Maryland, 20771*

*and Department of Astronomy, University of Maryland,*

*College Park, Maryland, 20742-2421*

(Dated: August 16, 2002)

## Abstract

I perform an independent analysis of radio Doppler tracking data from the Pioneer 10 spacecraft for the time period 1987–1994. All of the tracking data were taken from public archive sources, and the analysis tools were developed independently by myself. I confirm that an apparent anomalous acceleration is acting on the Pioneer 10 spacecraft, which is not accounted for by present physical models of spacecraft navigation. My best fit value for the acceleration, including corrections for systematic biases and uncertainties, is $(8.60 \pm 1.34) \times 10^{-8}$ cm s$^{-2}$, directed towards the Sun. This value compares favorably to previous results. I examine the robustness of my result to various perturbations of the analysis method, and find agreement to within $\pm 5\%$. The anomalous acceleration is reasonably constant with time, with a characteristic variation time scale of $> 70$ yr. Such a variation timescale is still too short to rule out on-board thermal radiation effects, based on this particular Pioneer 10 data set.

PACS numbers: 04.80.-y, 95.10.Eg, 95.55.Pe

---

[*] Electronic address: craigm@lheamail.gsfc.nasa.gov

## I. INTRODUCTION

Measurements of spacecraft motions in the solar system can be used as tests of gravitation and relativity. Recently, Anderson et al. [1, 2] have presented the discovery of an anomalous effect seen in radio tracking data from the Pioneer 10 spacecraft. When interpreted as a Doppler shift, this anomalous effect corresponds to a constant acceleration, directed towards the Sun, of approximately $(8 \pm 1) \times 10^{-8}$ cm s$^{-1}$. Anderson et al. (hereafter A02) found that the anomalous effect could not be explained by previously known physics or spacecraft properties.

The discovery of the anomaly has stimulated numerous efforts to explain it. Some of the explanations involve "new physics," such as modified gravity or dark matter, while other explanations invoke a change in the physical properties of the Pioneer spacecraft, such as a asymmetric radiation profile. I have considered a third avenue of exploration, which is to test the analysis procedure for flaws. In this paper, I present an independent analysis of the Pioneer 10 trajectory and search for an anomalous acceleration.

A02 studied radio tracking data from four deep space missions: Pioneer 10, Pioneer 11, Ulysses, and Galileo. All four of these missions showed suggestions of an anomalous acceleration of order $10^{-7}$ cm s$^{-2}$. However, A02 considered the determination of the anomalous acceleration of the Pioneer 10 spacecraft to be the most reliable. Therefore I have focussed exclusively on the Pioneer 10 data for my analysis. Once I had verified the presence of an anomalous acceleration, I tested the result for robustness in several different ways.

All of the procedures discussed in this paper were developed by myself [9] and written in the Interactive Data Language (IDL) [7, 8]. During the development I had only minimal contact with the A02 group authors, and as I detail below, these contacts had a minimal impact. Thus, I consider this work to be an independent test of the analysis by A02. I have analyzed a subset of the Pioneer 10 tracking data that is available from the public archives, which is, of course, the same data that A02 used in their analysis. The time coverage of my analysis (years 1987–1994) is most comparable to that of the original discovery presented in A02. By necessity, many of the analysis procedures I developed will be at least similar to those of A02, but I attempt to extend the analysis by considering additional models, including spacecraft spin, maneuvers, and time-variation of the anomalous acceleration.

The contents of the paper are as follows. Section II briefly describes the Pioneer 10

spacecraft and the Deep Space Network systems. Section III presents the methods I used to acquire the data and perform initial filtering, while Sec. IV describes the analysis and modeling techniques that I employed. The results of the tracking and uncertainty analyses are presented in Sections V and VI. This is followed by a short discussion and conclusion in Sections VII and VIII.

## II. SPACECRAFT AND COMMUNICATIONS

I provide only a cursory description of the Pioneer spacecraft, and Pioneer and DSN communications systems here. I refer the reader to A02, and references therein, for a more complete description.

### A. Pioneer 10 Spacecraft

Pioneer 10 was launched on 2 March 1972 and, after an encounter with Jupiter, has followed a hyperbolic escape trajectory from the solar system. On 1 January 1987, the spacecraft was approximately 40 A.U. from the Sun, and receding with a nearly constant velocity of 12.8 km s$^{-1}$.

The main physical features of the Pioneer 10 spacecraft are the parabolic high gain antenna, with a radius of 137 cm; the instrument compartment, which faces the direction of travel; and the two radioisotope thermoelectric generators (RTGs), which are attached to the compartment by booms of 300 cm length. The Pioneer 10 spacecraft is spin stabilized, and spins at a rate of $\simeq 5$ rpm. The spin axis is aligned with the high gain antenna axis, which is designed to point towards the Earth, opposite the direction of travel.

The transponder on board Pioneer 10 functions in the S-band. The uplink signal from Earth is received by the high gain antenna at 2.11 GHz, while the downlink signal to Earth is transmitted at a frequency close to $\nu_o = 2.292$ GHz. I have used only data where the spacecraft communications system was operated in "coherent" mode. In this mode, the spacecraft retransmits a downlink signal, phase-locked to the uplink, with an exact frequency turnaround ratio of 240/221.

3

## B. DSN Communications

Communications with Pioneer 10 are accomplished using the Deep Space Network (DSN). The DSN maintains antenna complexes at Canberra, Australia; Goldstone, California; and Madrid, Spain. Radio tracking observations are normally obtained in the course of mission operations for the purposes of spacecraft navigation. The two basic types of tracking are ranging, which directly measures the spacecraft distance via round trip light travel time; and Doppler, which measures indirectly the range rate, or relative velocity along the line of sight. Tracking passes were obtained more or less regularly spaced throughout the time range 1987–1994, and within individual years, although there were apparently some campaigns of more intensive tracking coverage.

During uplinks, a digitally controlled oscillator (DCO) is programmed to a precise frequency, which then drives the Exciter Assembly, whose signal is sent to the transmitting antenna. The uplink frequency is typically Doppler-compensated so that the frequency received by the spacecraft is near 2.11 GHz [3]. On the downlink leg, after being received at Earth, the Pioneer 10 Doppler signal is down-converted to a 1 MHz intermediate frequency. The Metric Data Assembly is used to accumulate a continuous count of Doppler cycles at this intermediate frequency, at fixed integration intervals. The Doppler count so computed represents the integrated range rate (i.e. the line of sight change in distance between the antenna and spacecraft). These quantities are typically differenced and, after further straightforward manipulations, produce the mean Doppler frequency over the integration interval [2, 4, 5].

Since the Pioneer spacecraft was 40–69 A.U. from the Earth for the period of this analysis, the round trip light travel time ranges from 11 to 16 hours. Thus, while it is possible for the same station to be used for both the uplink and downlink legs of the transmission to and from the spacecraft (known as "two-way" Doppler), it is more common for one station to transmit the uplink leg and a separate station to receive the downlink leg some hours later, which is known as "three-way" Doppler. As far as the analysis is concerned, both of these kinds of Doppler tracking data are identical and can be handled the same way.

For spacecraft ranging, a unique repeating ranging code is modulated onto the 2 GHz carrier wave. Upon return from the spacecraft, the received ranging code is correlated with the transmitted one, and a range time delay can be computed, modulo the period of the

ranging code pattern. No reliable range data were available for Pioneer 10, and so I analyzed only the Doppler tracking data.

## III. DATA PREPARATION

I obtained Pioneer 10 Doppler tracking data from the publicly accessible NSSDC archive. The JPL Radio Science group has submitted a substantial portion of the tracking data to the archive in the form of digital tapes which must be staged manually onto a computer disk. I requested data covering the time period 1987–1994. Data from beyond April 1994 is not available from NSSDC. In addition, there are a number of gaps in the data. The largest gap is due to an unreadable archive tape which covered the interval June 1990 to June 1991. The data are stored in a standard Archival Tracking Data File (ATDF) format [6].

An initial level of filtering and processing was applied to the raw ATDF records. A large number of records were in "one-way" Doppler mode (i.e., transmissions originating from the spacecraft) and were simply discarded. The integration time of the records was variable, and ranged from 0.1 s (so-called "high rate" Doppler), to $\sim 100$ s or more. The high rate data in particular contained a large number of samples, and to prevent over-weighting of those segments, I chose to accumulate the Doppler counts to intervals of at least 60 s in duration. I also eliminated discontinuous or noisy data, which occur preferentially at the beginnings and ends of tracking passes, or during noisy passes. A basic sliding 10-sample median filter was applied, and points more than 100 Hz from the median were discarded.

## IV. ANALYSIS OVERVIEW

The data consist of a time series of observed frequencies at designated DSN antennae. The dominant variations observed in the data are the annual signature of the Earth's motion in the solar system and the diurnal signature of the Earth's rotation. The diurnal term contains both the motions of the receiving and the transmitting antennae involved in the tracking pass. Finally, of course, there is the Doppler variation introduced by the Pioneer 10 spacecraft itself, which is the sought-after signal.

In this section, I will follow the terminology established by A02 in identifying epoch of transmission and reception. The epoch of transmission from the Earth is $t_1$, the epoch of

interaction of the signal with the Pioneer 10 spacecraft is $t_2$, and the epoch of reception back at the Earth is $t_3$. All of these times are referred to the Barycentric Dynamical Timescale (TDB), which is a coordinate time at the solar system barycenter. TDB is also the effective argument of the JPL planetary ephemerides. The 3-vectors $\mathbf{r}_1$, $\mathbf{r}_2$, and $\mathbf{r}_3$ represent the positions of the corresponding antenna at the corresponding epoch, and $\mathbf{v}_1$, $\mathbf{v}_2$, and $\mathbf{v}_3$ represent the velocities. The vector difference, $\mathbf{r}_{12}$, is defined as $\mathbf{r}_1 - \mathbf{r}_2$. These vector quantities are measured in the solar system barycenter frame.

The original station times in the ATDF records are referred to Coordinated Universal Time (UTC). When computing Earth rotation and orientation quantities, the Terrestrial Dynamical Time (TDT) timescale is used. Conversion between the UTC, TDT and TDB timescales is straightforward using standard practices [10, 11].

The expected frequency at the receiver at time $t_3$ can be expressed as

$$f_{3e} = [(240/221)(f_1 d_{12}) - \eta f_{\text{spin}}] d_{23} + \Delta\nu_{\text{path}}, \tag{1}$$

where $f_1$ is the uplink frequency at time $t_1$ as measured at the transmitter, $f_{\text{spin}}$ is the spacecraft spin frequency at time $t_2$, and the ratio $240/221$ is the spacecraft transponder turnaround ratio (note that $\eta = 1 + 240/221$). The factors $d_{12}$ and $d_{23}$ embody the Doppler shifts of the moving spacecraft and earthbound antennae. The frequency multiplier on the uplink leg is

$$d_{12} = \frac{\sqrt{1 - |\mathbf{v}_1|^2/c^2}}{(1 - \hat{\mathbf{r}}_{12} \cdot \mathbf{v}_1/c^2)} \frac{(1 - \hat{\mathbf{r}}_{12} \cdot \mathbf{v}_2/c^2)}{\sqrt{1 - |\mathbf{v}_2|^2/c^2}}, \tag{2}$$

where the first fraction represents the relativistic Doppler shift due to the Earth motion, and the second due to the spacecraft motion. The unit vector $\hat{\mathbf{r}}_{12}$ points from the transmitting station to the spacecraft, i.e., $\hat{\mathbf{r}}_{12} = \mathbf{r}_{12}/r_{12}$. The downlink factor, $d_{23}$, is constructed in the same fashion, by substituting $1 \to 2$ and $2 \to 3$.

The final term in equation 1, $\Delta\nu_{\text{path}}$, represents additional Doppler effects caused by small effective path length changes, aside from those due to geometric antenna motions. Generally speaking, this term can be written as $\Delta\nu_{\text{path}} = -2 \, dl/dt \, \nu_o/c$, where $dl/dt$ is the time rate of change of effective photon trajectory path length along the line of sight. The factor of 2 comes from the two legs of the round trip path.

In this paper I consider the effective path length due to the "Shapiro" delay [12]. The Shapiro delay reflects the extra proper distance traveled by a photon, beyond the classical

geometric distance, in the Sun's gravitational potential, as predicted by general relativity,

$$l_{\text{shap}} = (1 + \gamma)\frac{GM_\odot}{c^2}\ln\left[\frac{r_1 + r_2 + r_{12}}{r_1 + r_2 - r_{12}}\right], \tag{3}$$

where $\gamma$ is a parameter of the parameterized post-Newtonian formulation of gravity [13, 14]. For general relativity, $\gamma = 1$. On an annual timescale, the impact parameter of the photon trajectory increases and decreases, with a minimum distance of about $8 \times 10^6$ km. Conversion to a Doppler shift is achieved by numerically differentiating equation (3), which yields an annual signal with amplitude $\pm 150$ mHz. As discussed further below, I do not model the effects of the solar corona.

The known quantities are the receiver quantities $t_3$, $f_3$, and the station identification for each Doppler sample. In order to compute the expected frequency at the same epoch, all of $\mathbf{r}_{\{1,2,3\}}$ and $\mathbf{v}_{\{1,2,3\}}$ must be determined. This is especially important because even the time of transmission, $t_1$, and hence the transmission frequency, $f_1$, are not known *a priori*. Starting from the reception epoch, the spacecraft epoch $t_2$ is determined by solving the light travel time equation [8], $t_3 - t_2 = r_{23}/c + (l_{\text{shap}})_{23}$ via an iterative process, using the known trajectory and rotation properties of the Earth, and a trial trajectory of the spacecraft. In the same way, the transmission epoch $t_1$ can be determined. The ATDF data contains a special record of the transmitter configurations, including the frequency of the antenna's DCO, from which the transmitted frequency $f_1$ can be determined.

The motions of the Earth center are interpolated from the JPL DE405 planetary ephemeris [8, 22], which is referred to the axes of the International Celestial Reference Frame (ICRF). The position and velocity of Earth stations with respect to the geocenter, referred to an inertial coordinate system such as the ICRF, must take into account Earth rotation and the changes in Earth orientation parameters. The apparent sidereal time, which is the hour angle of the Earth referred to an inertial system, is taken from Aoki et al. [10, 16]. Earth precession and nutation describe the motion of the Earth rotation axis with respect to the celestial sphere. These parameters are determined based on the standard IAU 1976 (precession) and IAU 1980 (nutation) theories, and are expressed as a function of TDT. The nutation in obliquity and longitude are corrected using series provided by the International Earth Rotation Service (IERS [15]), which determines these angles to high precision via regular Very Long Baseline Interferometry (VLBI) observations of distant quasars. The polar motion with respect to the International Terrestrial Reference Frame (ITRF), and small

variations in the length of day (i.e., UT1−UTC) are also taken into account. Coordinates of earthbound DSN antennae, referred to the ITRF, are also known to centimeter precision or better based on VLBI, are taken from an existing DSN publication [18] (but see Sec. V).

## A.  Equations of Motion

The trajectory of the Pioneer 10 spacecraft must be determined by integrating the equations of motion over the time interval of interest, given a trial set of initial conditions. The equations of motion I used were

$$d\mathbf{v}/dt = \mathbf{a}_N + \mathbf{a}_S + \mathbf{a}_P$$
$$d\mathbf{r}/dt = \mathbf{v} \tag{4}$$

where $\mathbf{a}_N$ is due to Newtonian gravity, $\mathbf{a}_S$ is the acceleration due to solar radiation pressure; and $\mathbf{a}_P$ is an anomalous acceleration term (i.e., that which is not accounted for by known physics).

A02 considers additional terms for the acceleration which allow for alternate theories of gravity (their equation 3). I find that over the span of the data, these terms are always smaller than $3 \times 10^{-12}$ cm s$^{-1}$, and thus I neglect them for the purposes of Doppler tracking analysis. Other accelerations which I disregard: solar wind pressure ($< 10^{-13}$ cm s$^{-2}$); collisions with interplanetary dust ($< 10^{-12}$ cm s$^{-2}$, to heliocentric radii of 60 A.U. [19, 20]); and the gravitational attraction of the Kuiper belt ($< 3 \times 10^{-10}$ cm s$^{-2}$ [2]).

The Newtonian gravitational acceleration was computed as

$$\mathbf{a}_N = \sum_j \frac{GM_j(\mathbf{r}_j - \mathbf{r})}{|\mathbf{r}_j - \mathbf{r}|^3} \tag{5}$$

where $M_j$ and $\mathbf{r}_j$ are the mass and position of solar system body $j$, referred to the J2000 coordinate frame. The bodies included in the sum were the Sun, moon, and planets, the positions of which were interpolated from the JPL DE405 planetary ephemeris [8, 22].

In a manner similar to A02, I model the acceleration due to solar radiation pressure as radially directed outward from the Sun with a magnitude

$$a_S = \frac{\mathcal{K} f_\odot A_P}{c M_P} \left| \frac{1 \text{ A.U.}}{\mathbf{r} - \mathbf{r}_\odot} \right|^2 \cos\theta \tag{6}$$

where $\mathbf{r}_\odot$ is the barycentric position of the Sun, and the other constants in the equation are defined in Table I. For the Pioneer 10 geometric area I have used the area of the high gain antenna, which has a radius of 137 cm. The angle of the antenna to the Sun, $\theta$, is always less than 1.5° for Pioneer 10 after 1987, and here I have approximated it as $\theta = 0°$ with a loss in precision in acceleration of $< 4 \times 10^{-12}$ cm s$^{-1}$.

The Pioneer 10 anomalous acceleration, $\mathbf{a}_P$, is modeled primarily as a constant acceleration, $\mathbf{a}_P = a_P\hat{\mathbf{r}}$, where here $\hat{\mathbf{r}}$ is a unit vector pointing from the Sun to the spacecraft. As noted by A02 (and below), the Doppler tracking data for Pioneer 10 do not permit one to distinguish between a geocentric or heliocentric acceleration, so this representation is also equivalent to an acceleration directed along the Earth-spacecraft line. As I am using the "usual" sign convention for frequencies and velocities [17], a negative value for $a_P$ will represent an apparent acceleration towards the Sun.

I also test the constancy of the acceleration by adding a *jerk* term,

$$\mathbf{a}_P(t) = (a_P(0) + j_P t)\hat{\mathbf{r}} \tag{7}$$

where $j_P$ is the anomalous jerk, which measures the deviation of the acceleration from a constant. This expression can be rewritten as

$$\mathbf{a}_P(t) = a_P(0)(1 + t/T_{j_P}) \tag{8}$$

where $T_{j_P} = j_P/a_P(0)$ represents the timescale over which the anomalous acceleration changes. However, since the heliocentric spacecraft velocity is nearly constant with time (heliocentric radial velocity range of 13.1–12.6 km, with a mean of 12.8 km s$^{-1}$), the jerk term is also equivalent to a spatial gradient of the anomalous force, and equation 8 can also be rewritten as

$$\mathbf{a}_P(t) = a_P(0)(1 + r/R_{j_P}) \tag{9}$$

where r is the heliocentric distance and $R_{j_P} = j_P/(a_P(0)v_r)$ is the physical distance scale for variations in the acceleration.

## B. Spacecraft Maneuvers

The Pioneer 10 antenna is designed to point towards the Earth. As the spacecraft moves outward through the solar system, regular maneuvers must be made to adjust the spacecraft

9

attitude to maintain an Earth-pointing direction. The spacecraft has two thruster assemblies mounted on the rim of the high gain antenna, which are aligned with the antenna and spin axes. During the maneuvers, the thrusters execute several small pulses, with each thruster assembly firing in opposite directions. The spin axis is gradually precessed until a spacecraft feedback loop determines that the antenna axis is again pointed towards the Earth. According to A02, the maneuver duration is about 15 minutes.

In principle, the impulses from the thrusters are in opposite directions, and thus should impart no net change in velocity to the spacecraft. In practice, the control of the thruster nozzles is imperfect, and it is possible that a small velocity change will be imparted during the maneuver. In most cases, these velocity increments or decrements are directly visible in the Doppler tracking data (see Sec. V). I treated these velocity changes as adjustable parameters. For the $j$th maneuver, I modeled the velocity change as $\Delta \mathbf{v}_j = \Delta v_j \hat{\mathbf{r}}_j$ where $\Delta v_j$ is a free parameter and $\hat{\mathbf{r}}_j$ is a unit vector which points from the Earth to the spacecraft at the time of the maneuver.

The precise epochs of the maneuvers are not easily determined from the ATDF data available from the NSSDC archive. In principle these data should always be available, in a "high Doppler rate" mode, since maneuvers can only be performed during tracking passes. Unfortunately very little of the high rate data is present in the archive. Rather than guess at the maneuver epochs, I requested and obtained from the Anderson group a file which contained the epochs of the maneuvers as used in the CHASMP program [21]. However, the velocity increments and directions were determined by my own independent analysis.

Since the maneuvers are modeled with a single quantity, they determine the *mean* velocity shift per maneuver. Shorter time scale effects, like transient leakage from the thruster nozzles, will not be modeled. However, A02 found that transient effects were small, and I will not model them further. A02 provides a sample case of a maneuver from December 23, 1993. This data was also present in the NSSDC archive files, and I was able to verify that the behavior was very close to that described by A02.

## C. Spacecraft Spin

The downlinked tracking signal is affected by the spacecraft spin (equation 1). The nominal spin period is approximately 4.4 rotations per minute (rpm), however the actual

10

spin period has varied between between 4.25 and 4.55 rpm over the time span of the data considered in this paper. Like the maneuver data, it could be possible to determine the spacecraft spin from high rate Doppler data taken during precession maneuvers. Because this data was largely unavailable from the NSSDC archive, I also obtained a file from the Anderson group which contained a detailed Pioneer 10 spin period history [21]. These spin rate measurements come from a variety of sources [2], including the star sensor, the Imaging Photo Polarimeter, and the Doppler signal from precession maneuvers. During the analysis, I performed linear interpolation between tabulated points in the file.

While I did not determine the spin history independently, there are several mitigating factors. First of all, a spin rate of 4.55 rpm corresponds to an effective frequency shift of ∼75 mHz. As I will show, a signal of this magnitude could in principle be detectable against the Doppler noise, but it is much smaller by a factor of ∼ 40 than the signal due to the anomalous acceleration by 1994. Second, the more relevant quantity is how the spin rate *change* affects the Doppler frequency. For my data, the frequency shift due to the spin rate change is only ± 3 mHz, which is essentially undetectable. I checked these results by performing an analysis run where the spin rate was held fixed at its mean value, and also at zero, and the changes were negligible.

### D. Integration of Equations

The equations of motion were integrated using an Adams-Bashford-Moulton predictor corrector algorithm, based on the DDEABM [23] routine of the SLATEC library [24] (translated to IDL [8]). This integrator is of variable order (up to order 13) and adaptive step size. I adjusted the error control parameters so that frequency residuals were less than 0.1 mHz. The initial conditions were the initial spacecraft position and velocity referred to the solar system barycenter.

### E. Additional Filtering

Several additional data filtering criteria were applied, which relate to the effects of the Earth's troposphere and the Sun's corona on the Doppler signal. The Earth's troposphere is known to introduce an additional signal propagation delay on the order of tens to hundreds

11

of nanoseconds. This effect is strongly dependent on the elevation angle of the spacecraft to the horizon. At low elevation angles, the secant effect multiplies the tropospheric delay by several times. In addition, there are terms in the tropospheric delay which depend both on the season, and atmospheric conditions at the time of the observation. These effects are most readily seen in ranging experiments were signal delay directly corresponds to range error. For Doppler tracking data, the tropospheric effect enters more subtly, as the time derivative of the delay, since during a single tracking pass the spacecraft's apparent position will generally increase or decrease in elevation.

Using my best-fit model (see below), I divided the residuals into intervals based on their elevation angle at time of reception. Figure 1 shows the root mean squared (rms) residuals in each interval, and demonstrates that below $15°$ elevation there is a strong increase. While A02 chose to apply an elevation-dependent weighting function which included data at low inclinations, but at a reduced weight, I simply excluded points for which either the received or the transmitted elevation angle was smaller than $15°$.

The solar corona also affects the quality of the data. During solar conjunctions, the trajectory of photons passes within ten solar radii of the center of the Sun. Similar to the troposphere, the bulk solar corona introduces a variable delay of 0–1.7 $\mu$s. The derivative of this variation may be imprinted on the Doppler signal. However A02 found that the net effects of the solar corona were small, and ultimately ignored them. I constructed a similar coronal model to that of A02 and also found that the the net effects of the solar corona on the Doppler signal were small. However the solar corona is not a uniform medium. In addition to the net propagation delays due to the coronal plasma, there is a general increase in the Doppler noise. Figure 1 also shows a plot of the rms residuals as a function of the photon trajectory impact parameter. Clearly the noise is enhanced for impact parameters within $7 \times 10^{12}$ cm ($\simeq 0.5$ A.U.), and so I also elected to exclude any trajectories which passed within that region. The excluded segments are shown in Figure 3, labeled as "C."

Finally, I found that there were several segments of data that were particularly noisy, and also elected to exclude those from further analysis. These segments were from 14 to 29 September 1987, 18 January to 23 February 1992, and 13 March to 29 April 1992, and are shown in Figure 3, labeled as "N." I could not find a direct explanation for why these particular segments were of a lower quality than the others.

I should note that the exclusion of the segments mentioned above had a small effect on

12

the result. When, in a separate analysis, I included all of the data, the same value for the anomalous acceleration was reproduced to within 6%. However, because of the sensitivity of the least squares optimization technique to outliers, it is prudent to exclude highly noisy data which can significantly bias the result.

## F. Least Squares Optimization

The Doppler data were fitted to the model iteratively using a least squares technique. The fitting code is based upon MINPACK-1 [25, 26], but translated to IDL [8]. The free parameters are: (1) the position and velocity of the spacecraft at the initial epoch; (2) an anomalous acceleration; (3) velocity increments $\Delta v_j$ due to maneuvers (a total of 18 increments); and (4) in some cases a jerk term. The Earth station coordinates and velocities were also preliminarily considered to be free parameters. Upon completion of the fit, parameter uncertainties were estimated by adjusting the Doppler frequency uncertainties so that the $\chi^2$ value was equal to unity, and appropriately rescaling the parameter uncertainties derived from the covariance matrix of the fit. In addition to providing the parameter uncertainties, this method also provides an estimate of the variance of the Doppler residuals for a given model.

Since outliers can still be a problem, I gradually removed the outliers by applying a threshold filter. Initially the acceptance region for residuals was ±10 Hz around zero. As the fit steadily improved, I narrowed the acceptance region until I reached a minimum of ±60 mHz. The distribution of residuals for the best fit is shown in Figure 2. The distribution has a clear sharp peak ($1\sigma$ width of 4.2 mHz), with broad wings that extend at least to 30 mHz and beyond. Thus, the measured variance in the residuals will always be larger than 4.2 mHz, and depend largely on the size of the acceptance window. I decided that a ±60 mHz window was a reasonable compromise between too lax and too aggressive outlier removal.

A total of 312,116 Doppler records passed the preliminary filtering process described in Sec. III. I found this number of data points to be unwieldy to process simultaneously in core memory of a typical workstation computer, both in terms of memory consumption and processing time. I elected to literally decimate the data, taking only every tenth sample. This resulted in 31,211 raw records for the main processing runs. After application of the corona, tropospheric and low-noise selection criteria, a total of 23,852 or 76% of the records

remained. As a consistency check, I applied the same analysis to successive independent batches of 31,211 records drawn from the full pool of Doppler records. I found that each batch produced comparable results to the main batch. The distributions of parameter values from all ten batches were well matched by the error estimates taken from the rescaled covariance matrix, and therefore I have reasonable confidence that the covariance matrix produces appropriate statistical parameter uncertainties, even in the environment of outlier points.

## V. RESULTS

In my best fit model I can confirm the signature of a constant acceleration acting on the Pioneer 10 spacecraft. Figure 3 shows the best fit model with and without the anomalous term [17]. Table II shows the best fitting anomalous acceleration value, $a_P$, for various cases, as well as the inferred variance in the Doppler residuals. The best fitting value of $a_P$ for 1987–1994 is $(7.70 \pm 0.02) \times 10^{-8}$ cm s$^{-2}$, where the uncertainty is statistical only. It is clear that the Doppler residuals show an increasing trend. By the end of the data span in 1994, the frequency of the received Doppler signal is higher than expected by approximately $+2.7$ Hz in a single round trip.

The entry labeled "A02 Interval I" refers to the specific time intervals defined by A02. Interval I spans 3 January 1987 to 17 July 1990 and Interval II spans 17 July 1990 to 12 July 1992. A02 also considers a third interval which continues up to July 1998. Because my data set contains a large gap from 1990.5–1991.5, and no data beyond 1994.3, I consider it inappropriate to quote a value of $a_P$ in Intervals II and III for direct comparison to A02. A02 finds anomalous accelerations in Interval I of $8.02 \pm 0.01$ and $8.25 \pm 0.02$ for the SIGMA and CHASMP techniques, respectively ($\times 10^{-8}$ cm s$^{-2}$). Here I have used the weighted least squares values with no corona model, as these are the most comparable to my own. Generally, there is good agreement between the work of A02 and myself.

The best fit case was performed without a jerk term. When a jerk is included, the fit improves slightly (as judged by the reduction in the rms residuals), and the anomalous acceleration value increases by about 5%. The small fitted jerk value demonstrates that the anomalous acceleration is reasonably constant over time, even when allowing the maneuver parameters to vary.

14

I have included two fits with simplified spacecraft spin models. The first model, "Mean spin," assumes that the spacecraft spin remains constant at its mean value of 4.40 rpm. The second model, "No spin," assumes that the spacecraft has no spin at all. Both cases produce results that are essentially indistinguishable from the best fit case, with similar values of $a_P$ and similar qualities of residuals. Thus, while the spin data was not independently determined by myself, it has little impact on the final result. The reason that the zero spin solution does not contain $\sim 75$ mHz residuals is that these residuals are essentially constant, and can easily be absorbed into the other free parameters, such as the initial velocity vector and the maneuver velocity increments.

Taking this possibility to its logical extreme, one might surmise that the entire anomaly could be absorbed into the other free parameters. The next entry in Table II, "Only maneuvers," fixes $a_P = 0$ while allowing the other parameters to vary. I found that the anomaly is indeed absorbed into the maneuver velocity increments, as might be expected. However this possibility is not likely for several reasons. First, the rms residuals are considerably worse. If one were to take the "best fit" case as a good fit, i.e. a reduced $\chi^2$ value of unity, then the "only maneuvers" case would have a reduced $\chi^2$ value of 7.2, which is very unlikely statistically. The residuals also show systematic trends which actually *magnify* the Doppler discontinuities across maneuver epochs (Figure 4). Also, one would have to explain how a set of maneuvers, whose times are irregularly spaced, could produce a steady increase in the velocity of the craft over 7.5 years to within one percent. Finally, the maneuver velocity impulses must be significantly larger in magnitude than the "best fit" case by a factor of $\simeq 7.5$. For these reasons I believe that the "only maneuvers" case to be extremely unlikely.

The final entry in Table II is the case where no maneuvers are modeled, i.e. all of the $\Delta v_j$ are set to zero. Of course, Doppler discontinuities are clearly visible in this case (Figure 5), but they are (a) small compared to the anomaly, and (b) both positive and negative sign, compared to the anomaly which is unidirectional. This result shows that even without any modeling of spacecraft maneuvers, the anomaly is significantly detected, and although considerable effort was put into accurate maneuver modeling, even a crude model would have sufficed.

In all of the values cited in Table II, the positions and motions of the Earth stations were fixed to the values determined from VLBI [18]. [The station motions are due primarily to tectonic drift.] In another fit (not shown), I allowed the station coordinates to be free

parameters. I found that the fitted station coordinates converged to the quoted positions to within a few meters. Therefore, I left the stations fixed to their fiducial positions.

While A02 divided their data set into three separate intervals, I do not believe this approach to be appropriate for the abbreviated data set that I have access to. Therefore, in my discussion I quote the "best fit" value, which covers the entire 1987–1994 range.

A02 discovered annual and diurnal signatures in their residuals, which had amplitudes of approximately 10 mHz each. While the source was ultimately undetermined, A02 believed the periodic residuals to be due to previously unrealized errors in the tabulated solar system ephemerides, and therefore considered it to be a systematic uncertainty in the analysis. As can be seen in the bottom panel of Figure 3, I also detect modulations of the ∼annual residuals at a similar amplitude. I also consider this effect to be a systematic uncertainty.

Finally, I considered the geometric origin of the anomalous acceleration. As I have already mentioned, I assumed that the anomalous acceleration was directed toward the Sun. In a separate fit, I adjusted the equations of motion so that the acceleration was directed toward the instantaneous position of the Earth instead of the Sun. This change altered the Doppler residuals systematically by less than 0.5 mHz, and altered the best fit anomalous acceleration value by less than 2%. Thus, the center of acceleration could be either the Sun or the Earth and still be consistent with the data. [27].

## VI. ANOMALOUS ACCELERATION AND UNCERTAINTIES

A02 presented a comprehensive discussion of the systematic uncertainties associated with the determination of the anomalous Pioneer acceleration. I do not intend to repeat such a discussion, but instead will summarize and adjust it. A02 divided the uncertainties into three main categories: those generated external to the spacecraft, those generated on board the spacecraft, and computational uncertainties.

A02 estimated that the uncertainties associated with effects external to the spacecraft were essentially negligible, with an rms contribution of $\simeq 0.04 \times 10^{-8}$ cm s$^{-2}$. The largest estimated systematic uncertainties were associated with effects generated on board the Pioneer 10 spacecraft. A02 estimated the rms contribution of these effects to be $1.27 \times 10^{-8}$ cm s$^{-2}$, which included terms for the reflected heat from the RTGs; differential emissivity of the RTGs; non-isotropic radiative cooling of the spacecraft; gas leakage; and other smaller

effects. I adopt those values here.

The third category, computational uncertainties, were estimated to be $\simeq 0.35 \times 10^{-8}$ cm s$^{-2}$, and included terms for consistency of modeling ($\sigma_{\text{consist-model}}$) and the unmodeled annual and diurnal residuals. A02 was able to rely on their Interval III (July 1992–July 1998) for the most consistent determination of anomalous acceleration, but most of that data was not available to me. Thus the consistency between different models in my analysis will by necessity be less. For the purposes of this work, I will take $\sigma_{\text{consist-model}}$ to be one half of the range of anomalous acceleration determinations, or

$$\sigma_{\text{consist-model}} = 0.21 \times 10^{-8} \text{ cm s}^{-2}, \tag{10}$$

where, to be conservative, I have included the "extreme" cases in Table II (compare to a value of $0.13 \times 10^{-8}$ cm s$^{-2}$ determined by A02). Thus, the total estimated computational uncertainty is $\simeq 0.38 \times 10^{-8}$ cm s$^{-2}$. The combination of the uncertainties from all three categories, assuming they are are uncorrelated, is $\sigma_P = 1.34 \times 10^{-8}$ cm s$^{-2}$.

A02 also identified experimental "biases," which were other effects that would tend to systematically increase or decrease the anomalous acceleration from its experimentally determined value. For example, they estimated that the radio transmitter exerts a radiation force which accelerates the spacecraft at $1.10 \times 10^{-8}$ cm s$^{-2}$, directed away from the Sun. This acceleration would tend to *increase* the anomalous acceleration. Their final bias value, using the sign convention of this paper [17], is $b_P = -0.90 \times 10^{-8}$ cm s$^{-2}$, which I also adopt.

Clearly, the uncertainty in the determination of the anomalous Pioneer 10 acceleration is systematics-dominated and not statistics-dominated. Determination of the absolute jerk is therefore similarly dominated by systematic uncertainties. Formally, I take the upper limit to the absolute jerk to be

$$|j_P| < \sigma_P/T = 5.7 \times 10^{-17} \text{ cm s}^{-3}, \tag{11}$$

where $T$ is the data time span of 7.5 years. This upper limit is a factor of $\sim 1.5$ larger than the value determined in Table II. A more interesting quantity is the *relative jerk* (e.g., equation 8). The Doppler tracking data alone show a reasonably linear correlation with time, and hence require a small relative jerk. The effects of a jerk term would be strongest in the 1994–1998 time range of the A02 data set, but A02 did not see the effect. I will therefore still consider the jerk term shown in Table II, expressed relative to $a_P$, to be an

upper limit. This leads to

$$|j_P/a_P| = T_{j_P} > 70 \text{ yr} \tag{12}$$

and

$$R_{j_P} > 170 \text{ A.U.}, \tag{13}$$

which implies that the anomalous acceleration, if it varies, must do so on broad spatial or temporal scales.

For my determination of the anomalous acceleration I will assume that the jerk is zero, and hence use the "best fit" case of Table II. Following the terminology of A02, I label that experimentally determined quantity to be $a_{P(\text{exper})} = -7.70 \times 10^{-8}$ cm s$^{-2}$. After adding the bias value and assigning the systematic uncertainty, I arrive at

$$a_P = a_{P(\text{exper})} + b_P \pm \sigma_P \tag{14}$$

$$= (-8.60 \pm 1.34) \times 10^{-8} \text{ cm s}^{-2}. \tag{15}$$

## VII. DISCUSSION

My best value of the anomalous acceleration agrees quite closely with the value determined by A02 ($a_{P(\text{A02})} = (-8.74 \pm 1.33) \times 10^{-8}$ cm s$^{-2}$), although it should be pointed out that I have essentially adopted their error analysis estimates directly. The rms residuals of all of the "non-extreme" cases in Table II are of order 8 mHz. This variance level is half of the standard error of 15 mHz that A02 assigned to their Doppler data processing, and thus compares quite favorably with their result (despite the outliers).

The scope of this paper is to verify the Pioneer 10 anomalous acceleration by performing an independent analysis. I will however discuss briefly some implications for alternate explanations of the effect.

A02 mentions the Yukawa potential [28] as a candidate form of modified gravity,

$$U(r) = -\frac{GM}{r} \left( \frac{1 + \alpha e^{-r/\lambda}}{1 + \alpha} \right) \tag{16}$$

where $\alpha$ and $\lambda$ are adjustable parameters. Upon computing the gradient of this potential and expanding in a power series of heliocentric radius $r$, one finds

$$a(r) = -\frac{GM}{r^2} + \left( \frac{\alpha}{1 + \alpha} \frac{GM}{2\lambda^2} \right) \left[ 1 - \frac{2}{3} \frac{r}{\lambda} \right] \tag{17}$$

18

where the first term is the Newtonian acceleration. The second term has a clear analogy to equation 9, where $a_P(0)$ is the term in parentheses, and the length scale $\lambda = 2R_{j_P}/3 > 110$ A.U. Thus, if the Yukawa acceleration — or any other modified-gravity acceleration — were to deviate from Newtonian plus a constant, this deviation would occur over spatial scales larger than the planetary solar system.

The anomalous acceleration has been proposed to be caused by radiation from the RTGs or electronics in the instrument compartment [29–32]. All electric power on-board is derived from the RTGs, which in turn derive their power from radioactive decay of $^{238}$Pu, with a half-life of $\tau = 87.74$ yr. This radioactivity also produces considerable waste heat of approximately 2000 W. As little as 63 W of electromagnetic radiation, if radiated directionally away from the Sun, could explain the anomalous effect. A02 has advanced several arguments against these classes of explanations for the anomaly. One argument is that the anomaly is well enough determined over time that the radioactive decay of $^{238}$Pu should be detectable, but is not. If the acceleration were related to heat dissipation, then its functional form would be

$$a_P = a_P(0)2^{-t/\tau} \simeq a_P(0)(1 - t\ln 2/\tau). \tag{18}$$

This equation is again a direct analog of equation 8, however with the constraint that $\tau = T_{j_P}\ln 2 > 50$ yr. This limit still accommodates the half-life of $^{238}$Pu, so an explanation based on radiation from the RTGs cannot necessarily be excluded by my analysis of the 1987–1994 Pioneer 10 data [33].

If the Doppler errors are considered to be approximately constant over time, then the error in the jerk should scale as $T^{-2}$, so additional data over a longer baseline could and should be much more constraining. A02 considered the constancy of the anomalous acceleration by dividing the data into three separate intervals, and attempting to analyze the intervals independently of one another. They found a variation of 2.0–5.1% between their Intervals I and III. The "jerk" solution I present here would produce a variation in the acceleration between the midpoints of the two intervals of about 8%, a value which is not unreasonably inconsistent with the results of A02.

In order to test the sensitivity to a jerk term, I performed a test using simulated data. I used the best fit trajectory *with jerk* to construct a synthetic Doppler series, without noise, over an 11.5 year baseline on a regularly sampled time grid. I then fitted that series to a model with *no jerk*, but including maneuvers. I found that a reasonably good fit could

be found. The rms residuals were $\sim 1$ mHz, which is much smaller than the typical rms residuals of the actual best fit models. The signature of the jerk was a small parabolic curve in the residuals in each segment between maneuvers. Thus, I consider it possible that a jerk term could be present in the residuals without being readily apparent. An analysis of the full Doppler data set would be desirable.

## VIII. CONCLUSION

I have confirmed by independent analysis that the Pioneer 10 anomalous acceleration exists in the Doppler tracking data, and is likely not to be an artifact of the software processing by A02. Direct comparison to A02's SIGMA acceleration value in their Interval I yields agreement at better than the 1% level. The anomaly is robust to different choices of spacecraft spin model, and also produces a consistent value even when all maneuvers are removed. This data does not constrain whether anomalous acceleration is geocentric or heliocentric. By including a jerk term, I have showed that the acceleration is reasonably constant as a function of time over a 7.5 year time baseline, but not constant enough to rule out thermal radiation effects due to radioactive decay of Plutonium on board the spacecraft.

---

[1] J. D. Anderson, P. A. Laing, E. L. Lau, A. S. Liu, M. M. Nieto, and S. G. Turyshev, Phys. Rev. Lett. **81**, 2858 (1998)

[2] J. D. Anderson, P. A. Laing, E. L. Lau, A. S. Liu, M. M. Nieto, and S. G. Turyshev, Phys. Rev. D, **65**, 082004 (2002) (A02)

[3] The Doppler compensation of the uplink signal largely accounts for the annual motion of the Earth, for which only a crude orbit prediction is required. This compensation does not disrupt the determination of the anomalous acceleration, since the relevant quantity is always the *difference* between the received and transmitted frequency.

[4] D. D. Morabito and S. W. Asmar, *The Telecommunications and Data Acquisition Progress Report*, 42–120, 121 (1994) (`http://tmo.jpl.nasa.gov/tmo/progress_report/`)

[5] T. D. Moyer, *Formulation for Observed and Computed Values of Deep Space Network (DSN) Data Types for Navigation*, JPL Publication 00-7 (October 2000).

[6] DSN Tracking System Interfaces, Archival Tracking Data File Interface, TRK-2-25, DSN Document 820-13, Rev. A (NASA, Washington D.C., 1988) (Mark IVA Implementation)

[7] Research Systems Incorporated, *IDL Reference Guide: IDL Version 5.4*, (Research Systems, Boulder, Colorado, 2000)

[8] Many of the IDL programs that I used in the analysis presented in this paper are available from my personal web page at `http://cow.physics.wisc.edu/~craigm/idl/idl.html`.

[9] While spacecraft tracking analysis and orbit determination is performed by the Flight Dynamics Facility at Goddard Space Flight Center, I am not affiliated with that group.

[10] P. K. Seidelmann, ed., *Explanatory Supplement to the Astronomical Almanac* (University Science Books, Mill Valley, CA, 1992).

[11] L. Fairhead and P. Bretagnon, Astron. Astrophys., **229**, 240 (1990)

[12] I. I. Shapiro, M. E. Ash, R. P. Ingalls, and W. B. Smith, Phys. Rev. Lett. **26**, 1132 (1971)

[13] C. M. Will, *Theory and Experiment in Gravitational Physics*, (Rev. Ed.) (Cambridge University Press, Cambridge, 1993).

[14] C. M. Will and K. Nordtvedt, Jr, Astrophys. J. **177**, 757 (1972).

[15] The IERS data file was found at `ftp://maia.usno.navy.mil/ser7/finals.all`, which contains series for Earth polar motion coordinates, nutation corrections, and the UT1-UTC deviation for May, 1976, to the present.

[16] S. Aoki, B. Guinot, G. H. Kaplan, H. Kinoshita, D. D. McCarthy, P. K. Seidelmann, Astron. Astrophys., **105**, 359 (1982).

[17] A02 distinguishes between the "usual" and "JPL" sign conventions for presenting frequencies

and velocities. In this paper, all quantities are presented using the "usual" convention. Higher frequencies are more positive; lower frequencies are more negative. A receding spacecraft has a positive velocity; an approaching one has a negative velocity.

[18] W. M. Folkner, *The Telecommunications and Data Acquisition Progress Report*, 42-128, 1 (1997) (http://tmo.jpl.nasa.gov/tmo/progress_report/)

[19] M. Landgraf, J.-C. Liou, H. A. Zook, and E. Grün, Astrophys. J. **123**, 2857 (2002)

[20] D. A. Gurnett, J. A. Ansher, W. S. Kurth, and L. J. Granroth, Geophys. Res. Lett. **24**, 3125 (1997)

[21] The epochs of precession maneuvers and the spacecraft spin history were kindly provided by Slava Turyshev of the A02 collaboration.

[22] E. M. Standish, Jr., *JPL Planetary and Lunar Ephemeris, DE405/LE405*, Jet Propulsion Laboratory Internal IOM No. 312.F-98-048 (1998).

[23] L. F. Shampine, and H. A. Watts, Sandia National Laboratory Report No. SAND79-2374 (Albuquerque, New Mexico, 1979)

[24] SLATEC library (Sandia, Los Alamos, Air Force Weapons Laboratory Technical Exchange Committee), available at http://www.netlib.org/slatec/

[25] Moré, Jorge J., in *Numerical Analysis*, Lecture Notes in Mathematics, vol. 630, edited by G. A. Watson (Springer-Verlag, Berlin, 1977), p. 105

[26] Moré, Jorge J., Argonne National Laboratory Report No. ANL-80-74 (Argonne, Illinois, 1980)

[27] For completeness I also tested whether the center of acceleration could be any other planet. I found that any of the inner planets (Mecury through Mars) could be the center without producing significantly different Doppler residuals. I believe this is because the inner planets orbit quickly enough that any component of the acceleration directed away from the sun is averaged to zero over the Doppler timespan. If, on the other hand, the center of acceleration were a fixed point in the solar system, then such averaging doesn't occur, and the fixed point would therefore need to be within $\sim 0.5$ A.U. of the Sun to be consistent with the Doppler data. I thank Slava Turyshev for suggesting this analysis.

[28] M. M. Nieto and T. Goldman, Phys. Rep. **205**, 221 (1991); **216**, 343 (1992).

[29] J. I. Katz, Phys. Rev. Lett. **83**, 1892 (1999).

[30] E. M. Murphy, Phys. Rev. Lett. **83**, 1890 (1999).

[31] J. D. Anderson, P. A. Laing, E. L. Lau, A. S. Liu, M. M. Nieto, and S. G. Turyshev, Phys.

Rev. Lett. **83**, 1891 (1999).

[32] L. K. Scheffer, (a) eprint gr-qc/0106010, the original modification; (b) eprint gr-qc/0107092; (c) eprint gr-qc/0108054.

[33] Similar reasoning can be made regarding explanations which invoke thermal radiation from the electronic components, since the electric power output of the RTGs has also been decreasing on a ~decade timescale (see Figure 16 of A02).

## TABLE I: Adopted Pioneer 10 and Solar Parameters

| Parameter | Value |
|---|---|
| Pioneer 10 Mass, $M_P$ (g) | $2.51883 \times 10^5$ |
| Pioneer 10 Area, $A_P$ (cm$^2$) | $5.90 \times 10^4$ |
| Solar Radiation Constant, $f_\odot$ (erg cm$^{-2}$ s$^{-1}$) | $1.367 \times 10^6$ |
| Reflectivity Coefficient, $\mathcal{K}$ | $1.77$ |

## TABLE II: Pioneer 10 Anomalous Acceleration (Various Procedures)

| Description | $a_P$ | RMS residuals[a] |
|---|---|---|
| | $10^{-8}$ cm s$^{-2}$ | mHz |
| Best fit | $-7.70 \pm 0.02$ | 7.9 |
| A02 Interval I | $-7.98 \pm 0.02$ | 7.1 |
| With jerk ($j_P = (+3.7 \pm 0.2) \times 10^{-17}$ cm s$^{-3}$) | $-8.13 \pm 0.02$ | 7.8 |
| Mean spin ($f_{\rm spin} = 4.40$ rpm) | $-7.72 \pm 0.02$ | 7.9 |
| No spin ($f_{\rm spin} = 0$) | $-7.74 \pm 0.02$ | 7.9 |
| Only maneuvers ($a_P = 0$) | $0.00$[b] | 21.3 |
| No maneuvers ($\{\Delta v_j\} = 0$) | $-8.10 \pm 0.01$ | 30.2 |

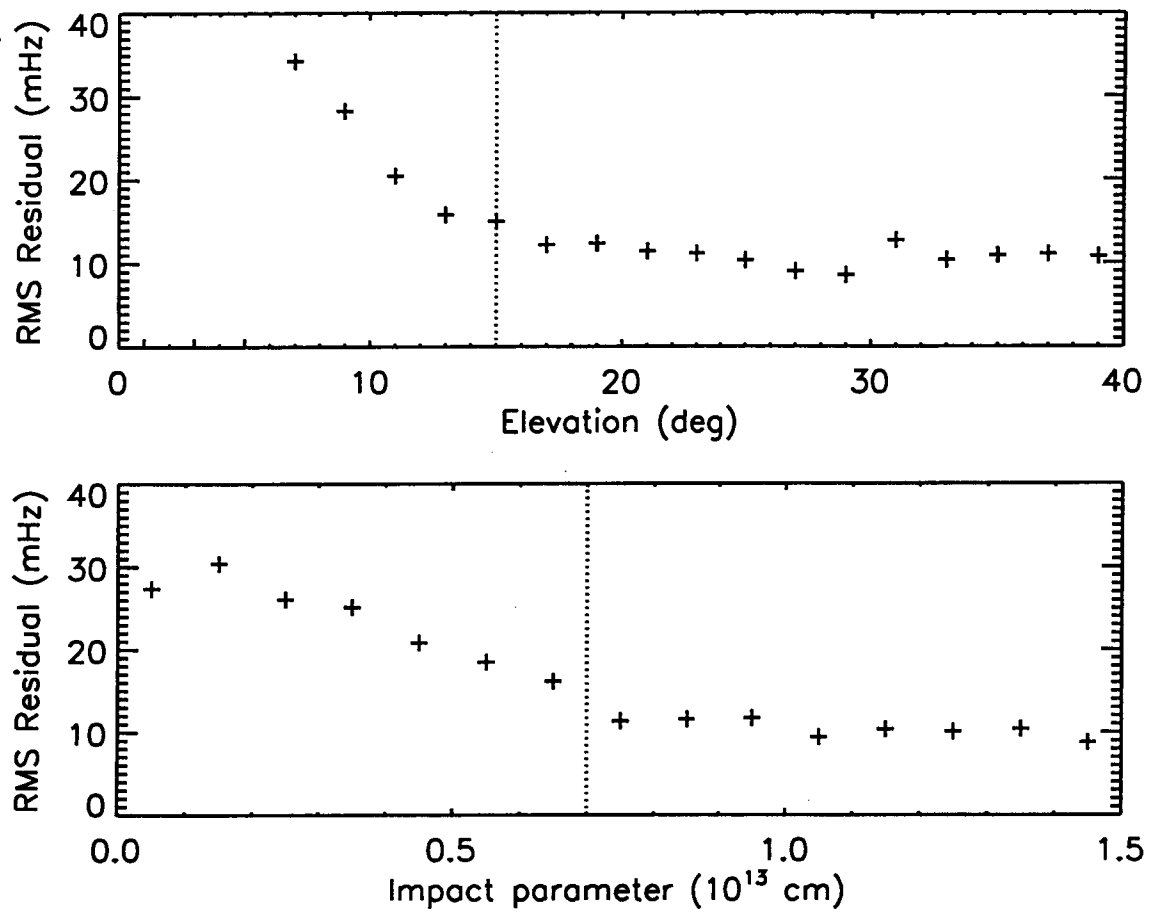[a]Assumes a window of $\pm 60$ mHz

[b]Parameter was fixed

FIG. 1: Plot of RMS residuals as a function of elevation of spacecraft above Earth horizon at time of reception (top) and as a function of point of nearest approach to the Sun of the photon trajectories (bottom). Data to the right of the vertical dotted line were used in the final analysis.
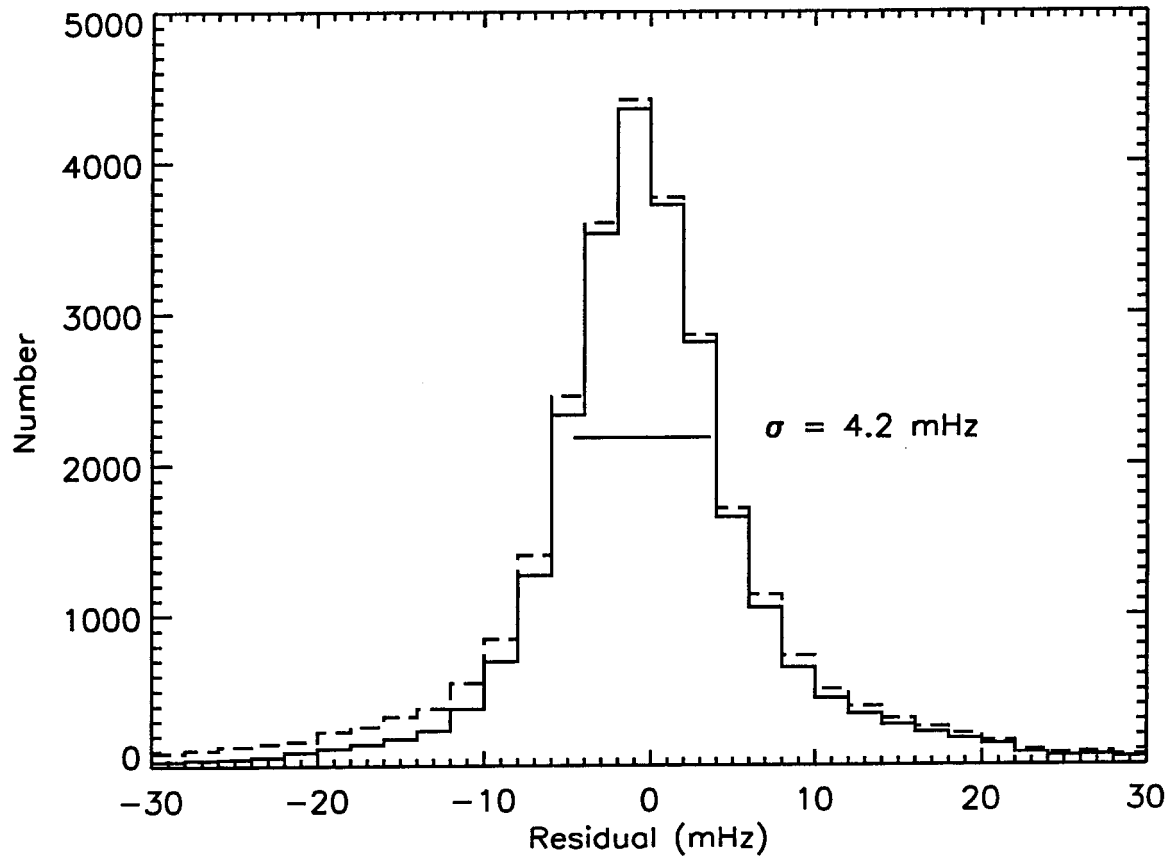
FIG. 2: Distribution of residuals of the best fit model for only the filtered data (solid line) and for all of the data (dashed line). The curve is characterized by a sharp central peak, well fit by a Gaussian with the width shown. The distribution contains significant tails.
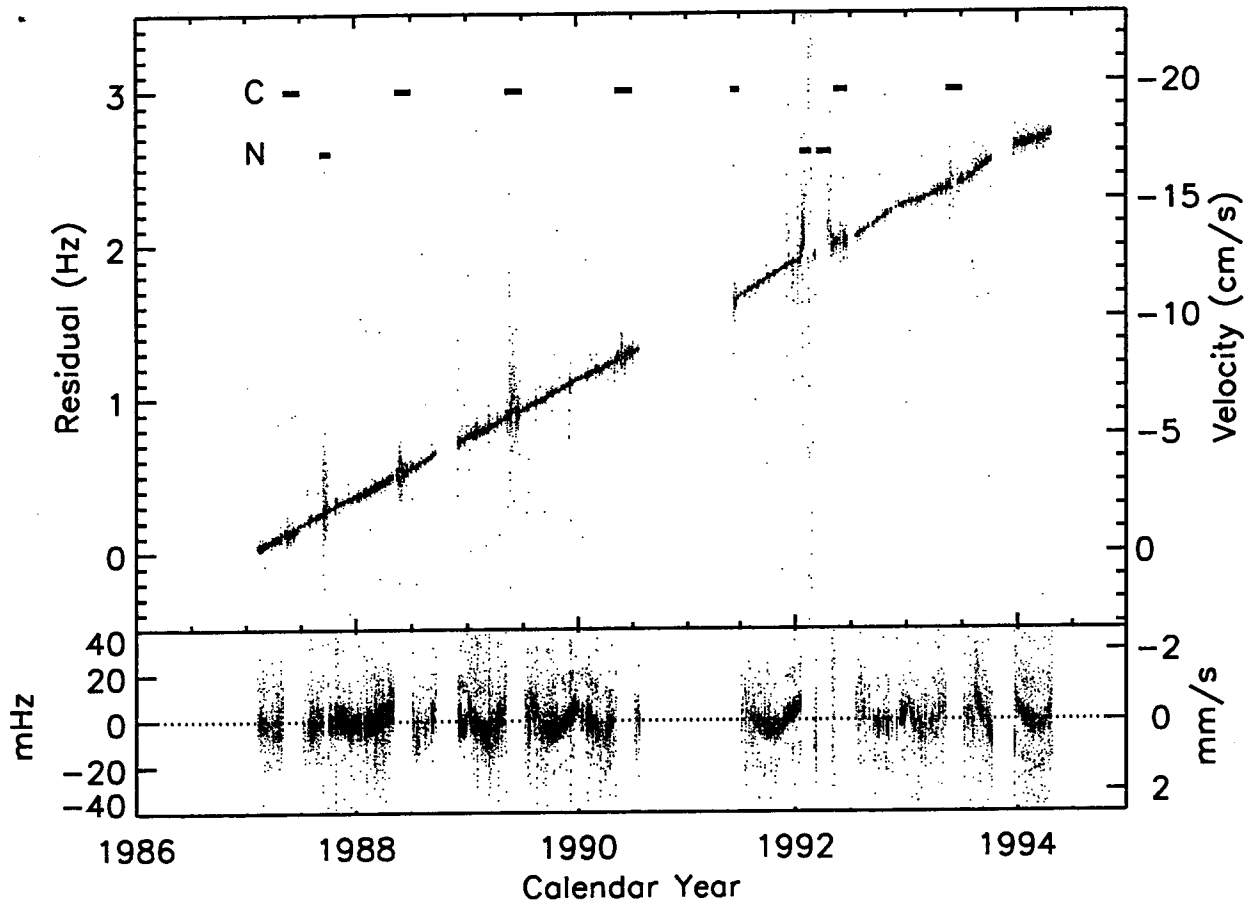
FIG. 3: Doppler residuals as a function of time of the best fit model. The top panel shows the residuals after setting $a_P = 0$, and demonstrates the linear increase with time. The top panel shows all of the data, including segments that were filtered out because of interference due to the solar corona (designated by a horizontal bar with "C") or due to general noise (designated "N"; see text). The bottom panel shows the filtered residuals, including the best fit value of the anomalous acceleration. The equivalent spacecraft velocity is also shown. Velocities and frequencies are plotted using the "usual" sign convention [17].
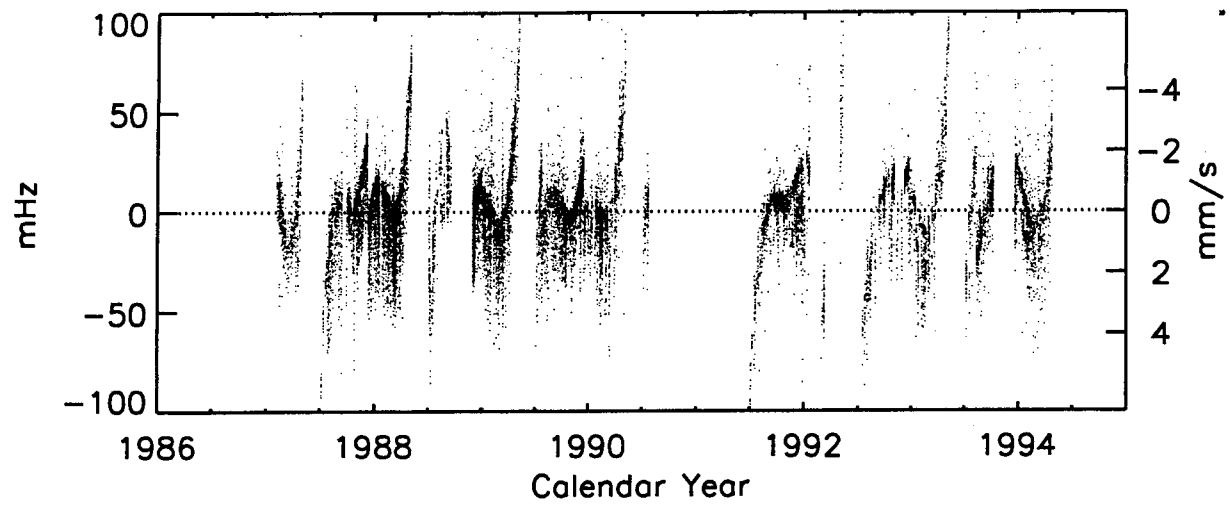
FIG. 4: Doppler residuals as a function of time of the "only maneuvers" case, showing how the maneuver parameters can absorb some but not all of the anomaly when $a_P$ is set to zero. Note the change in vertical scale from the bottom panel of Figure 3.
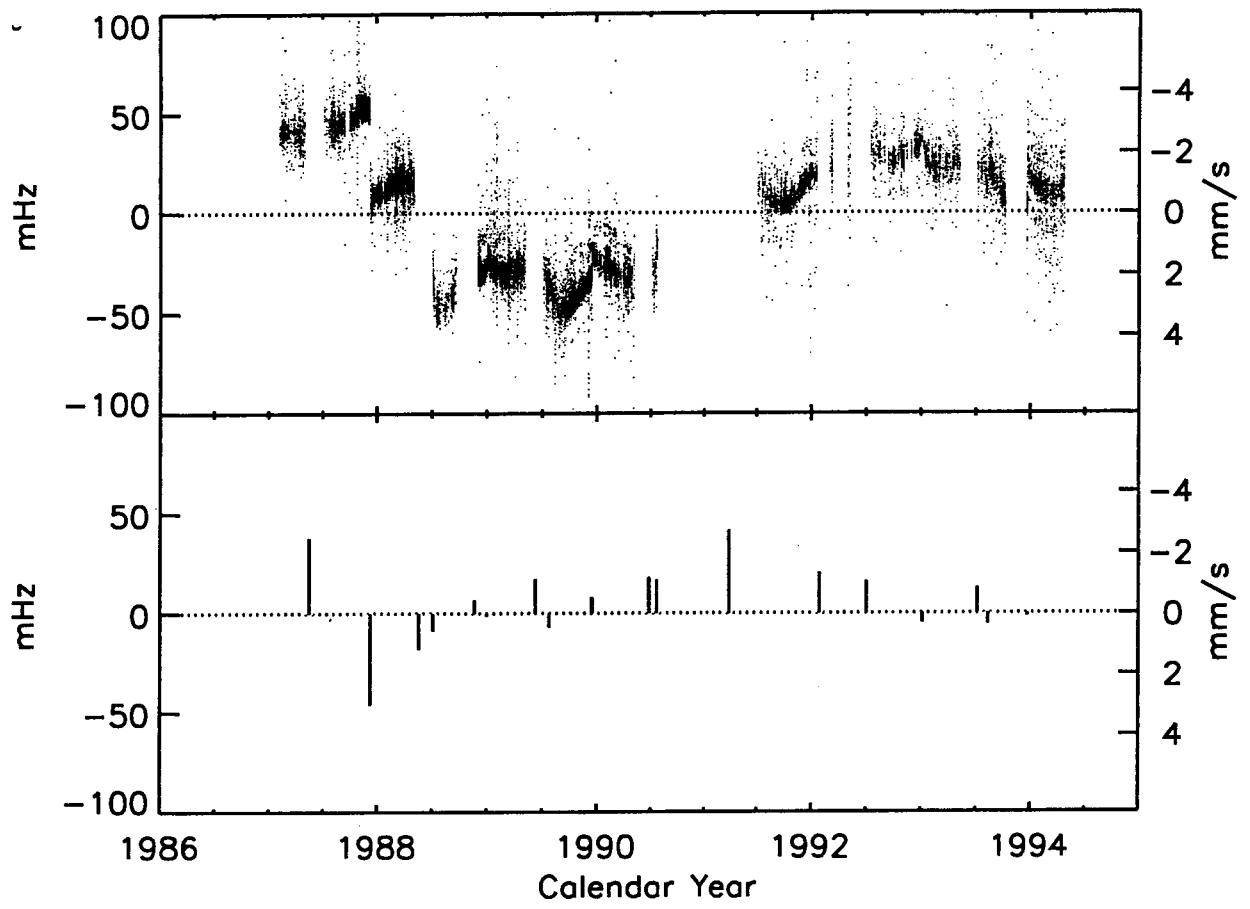
FIG. 5: Doppler residuals as a function of time for the "no maneuvers" case (top panel), showing that the Doppler shifts of the maneuvers are visible, but are small in comparison to the overall anomaly. The bottom panel shows the fitted velocity increments for the best fit case.